Journal of Pharmaceutical Sciences 105 (2016) 705–713

Contents lists available at ScienceDirect

Journal of Pharmaceutical Sciences

journal homepage: www.jpharmsci.org

Pharmaceutics, Drug Delivery and Pharmaceutical Technology

Mechanism of Decarboxylation of Pyruvic Acid in the Presence of Hydrogen Peroxide

Antonio Lopalco [1], Gautam Dalwadi [1], Sida Niu [1], Richard L. Schowen [1], Justin Douglas [2], Valentino J. Stella [1, *]

[1] Department of Pharmaceutical Chemistry, The University of Kansas, Lawrence, Kansas 66047
[2] Nuclear Magnetic Resonance Laboratory, Lawrence, Kansas 66045

ARTICLE INFO

Article history:
Received 20 May 2015
Revised 10 August 2015
Accepted 26 August 2015
Available online 30 September 2015

Keywords:
pyruvic acid
antioxidants
hydrogen peroxide
UV/Vis spectroscopy
peroxide scavenger
kinetics
NMR spectroscopy
chemical stability
hydration
mathematical model

ABSTRACT

The purpose of this work was to probe the rate and mechanism of rapid decarboxylation of pyruvic acid in the presence of hydrogen peroxide (H_2O_2) to acetic acid and carbon dioxide over the pH range 2–9 at 25°C, utilizing UV spectrophotometry, high performance liquid chromatography (HPLC), and proton and carbon nuclear magnetic resonance spectrometry (^{1}H, ^{13}C-NMR). Changes in UV absorbance at 220 nm were used to determine the kinetics as the reaction was too fast to follow by HPLC or NMR in much of the pH range. The rate constants for the reaction were determined in the presence of molar excess of H_2O_2 resulting in pseudo first-order kinetics. No buffer catalysis was observed. The calculated second-order rate constants for the reaction followed a sigmoidal shape with pH-independent regions below pH 3 and above pH 7 but increased between pH 4 and 6. Between pH 4 and 9, the results were in agreement with a change from rate-determining nucleophilic attack of the deprotonated peroxide species, HOO^-, on the α-carbonyl group followed by rapid decarboxylation at pH values below 6 to rate-determining decarboxylation above pH 7. The addition of H_2O_2 to ethyl pyruvate was also characterized.

Introduction

The purpose of this work was to probe the pH dependence of the reaction rates, as well as the mechanism of rapid decarboxylation of pyruvic acid in the presence of hydrogen peroxide (H_2O_2). The physicochemical properties (hydration equilibrium and dissociation) of pyruvic acid as well as a series of other α-ketocarboxylic acids was examined in an earlier study.[1] Here, the fast kinetics and mechanism of decarboxylation of pyruvic acid in the presence of H_2O_2 were studied at 25°C using a UV spectrophotometry technique and HPLC and nuclear magnetic resonance (NMR) product analysis. A mechanism of reaction, involving the tetrahedral intermediates (2-hydroperoxy-2-hydroxypropanoate[2]) (Scheme 1), was proposed that could explain the pH-rate profile.

The decarboxylation of pyruvic acid and a few other α-ketocarboxylic acids in the presence of peroxides has been studied earlier by others.[2-4] Most of these studies were incomplete or probed only in a narrow pH range. The novel use of carbon isotope effect on the decarboxylation by Melzer and Schmidt[4] suggested the possibility of a change in rate-determining step in the reaction but how this affected the pH-rate profile was not specifically examined. Hence, important mechanistic details of the reaction between pyruvic acid and H_2O_2 remain obscure.

Hydrogen peroxide and other peroxide species, such as organoperoxides (ROOR′) or hydroperoxides (ROOH), are reactive impurities present in many pharmaceutical excipients.[5] These peroxides may be introduced into excipients during the manufacturing process[6] or their concentrations could increase under storage conditions when exposed to oxygen.[7] Stability of active pharmaceutical ingredients is often compromised by these reactive peroxide species, examples of which appear throughout the literature.[7-13] Polymeric excipients, in particular, such as povidone,[7] crospovidone,[14] hydroxypropylcellulose,[6] polysorbate 80,[8-10] and polyethylene oxide,[15] are major sources of peroxides.

Peroxides can impact drug product stability by several mechanisms.[16] Peroxides can contribute to three types of oxidative

* *Correspondence to:* Valentino J. Stella (Telephone: +785-864-3755; Fax: +785-864-5736).
E-mail address: stella@ku.edu (V.J. Stella).

http://dx.doi.org/10.1002/jps.24653
0022-3549/

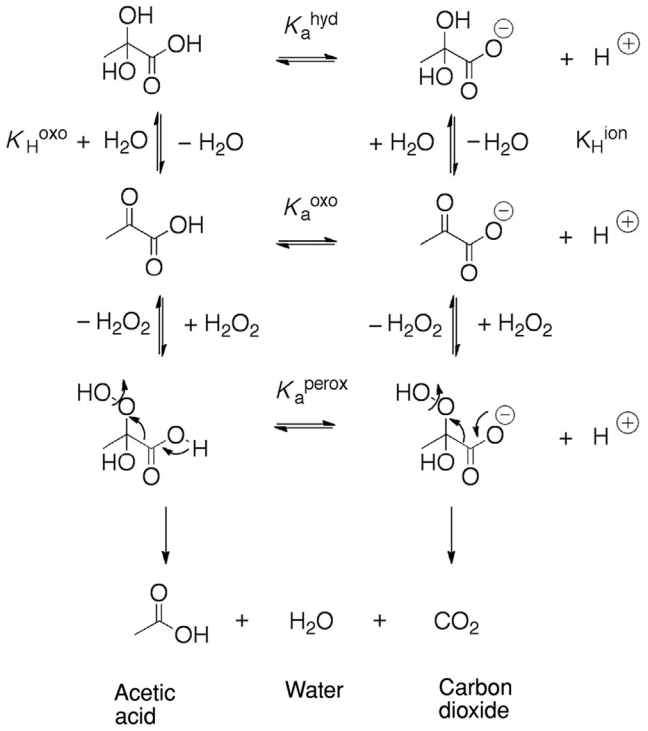

Scheme 1. Proposed overall reaction and ionization scheme involving the reaction of various pyruvic acid specie with H_2O_2.

chemical reactions with drugs: nucleophilic addition, electrophilic displacement, and radical reactions.[17] Therefore, it is important to remove peroxides during the manufacturing and before the packaging processes as well as preserve the stability of formulations during the storage using scavenger antioxidants.[6,7,17] Pyruvic acid is an excellent H_2O_2 scavenger.

It is also known that several endogenous or exogenous molecules in our body, such as cysteine, glutathione, methionine, ascorbic acid, and α-keto acids, including pyruvic acid, alter oxidation of proteins and important cellular components caused by H_2O_2 and reactive oxygen species.[18]

Materials and Methods

Materials

Sodium pyruvate ReagentPlus (≥99%), acetic acid ACS reagent (≥99.7%), sodium acetate 99%, H_2O_2 50% solution in water, sodium chloride BioXtra ≥99.5%, HCl 37% A.C.S. reagent, and dimethyl sulfoxide d_6 (DMSO d_6) 99.96% were commercially available from Sigma-Aldrich (Milwaukee, WI) and used without purification. NaOH certified A.C.S. pellets, NaH_2PO_4 H_2O, and Na_2HPO_4 anhydrous certified A.C.S. were purchased from Fisher Scientific (Fair Lawn, NJ). Tris-HCl +99% was commercially available from Acros Organic (NJ). Deionized water was used to prepare all the samples for the UV, NMR, and HPLC analysis.

Methods

UV Spectophotometric Analysis

Separate sodium pyruvate (1.5 mM) and H_2O_2 solutions with concentrations between 5 and 30 mM were prepared using buffers tris (pH 9), phosphate (pH 6-8.0), and acetate (pH 4.0-5.5) at 20 and 40 mM and HCl 0.01 and 0.003M, with ionic strength adjusted to 0.15 with NaCl. Equal volume of the pyruvate solution was mixed with each H_2O_2 solution in a quartz cuvette (Starna Cells, Inc., Atascadero, CA) equilibrated at 25°C in a water bath. Even though H_2O_2 and pyruvic acid absorbed at the similar wavelengths, it was possible to monitor the overall drop in absorbance at 220 nm as pyruvate was consumed by H_2O_2 (Scheme 1) to form acetic acid and CO_2. A UV spectrophotometer Spectramax® PLUS^{384} (Sunnyvale, CA) was used to monitor the fast kinetics.

HPLC Analysis

A Shimadzu SIL 10-A system including a SIL-10A autoinjector, a SPD-10A UV–Vis detector, a SCL-10A system controller, LC-10AT pumps, and Class-VP version 4.10 software obtained from Shimadzu Scientific Instruments (Columbia, MD) was used. A Phenomenex Synergi 4 μm Hydro-RP 80 Å 250 × 4.6 mm^2 column thermostated at 30°C was used. An isocratic separation was performed using 25 mM NaH_2PO_4 with pH 3 as mobile phase at a flow rate of 0.7 mL/min. The UV detection of pyruvic acid and acetic acid (the degradation product) was carried out at 220 nm. An injection volume of 5 μL was used in all experiments.

^{1}H, ^{13}C-NMR, Heteronuclear Single Quantum Correlation, and Heteronuclear Multiple Bond Correlation

The starting concentration of sodium pyruvate and ethyl pyruvate were 150 mM, and the concentration of H_2O_2 was 450 mM. Equal volumes of 0.25 mL of sodium pyruvate and H_2O_2 solutions both at pH 2 and ionic strength 0.15 with sodium chloride were mixed in a 5-mm NMR tube and the spectra were acquired. Ethyl pyruvate and H_2O_2 solutions were also titrated to the desired pH 5 using concentrated hydrochloric acid such that the final ionic strength was 0.15 with sodium chloride. Equal volumes of 0.25 mL of each solution were mixed in a 5-mm NMR tube and the spectra were acquired. The pH of each sample was measured directly in the NMR tube using a 5 mm pH electrode purchased from Wilmad Labglass (Vineland, NJ). The samples of ethyl pyruvate in presence of H_2O_2 and sodium pyruvate alone were stable during the analysis and no variation in spectra and pH values was observed when the runs were repeated. 1D and 2D ^{1}H and ^{13}C NMR spectra were acquired on a 500-MHz Bruker AVIII spectrometer (Rheinstetten, Germany) equipped with a carbon-enabled cryoprobe. Sample temperature was set to 25°C. For kinetics experiments, the Bruker automation program "multi_zgvd" was employed to acquire 1D ^{13}C spectra (64 scans) every 3 min until the reaction was judged complete. The following parameters were used for 2D ^{1}H-^{13}C heteronuclear single quantum correlation (HSQC) experiment: number of scans, 1; number of complex data points (experiments) in F1, 148; number of complex data points in F2, 512; sweep width in F1 and F2, 165 and 16 ppm, respectively; spectrometer offset for ^{1}H and ^{13}C, 4.7 and 70 ppm, respectively; and interscan delay, 2 s. The following parameters were used for 2D ^{1}H-^{13}C heteronuclear multiple bond correlation (HMBC) experiment: number of scans, 2; number of complex data points (experiments) in F1, 128; number of complex data points in F2, 2048; sweep width in F1 and F2, 222 and 13 ppm, respectively; spectrometer offset for ^{1}H and ^{13}C, 6 and 100 ppm, respectively; interscan delay, 1.5 s. Data were processed with the software MestreNova (MestreLab Research S. L., Santiago de Compostela, Spain). For 2D, spectra were zero filled to 512 data points in the indirect dimension and multiplied by cosine-square apodization function in both dimensions prior to Fourier transform and phase correction.

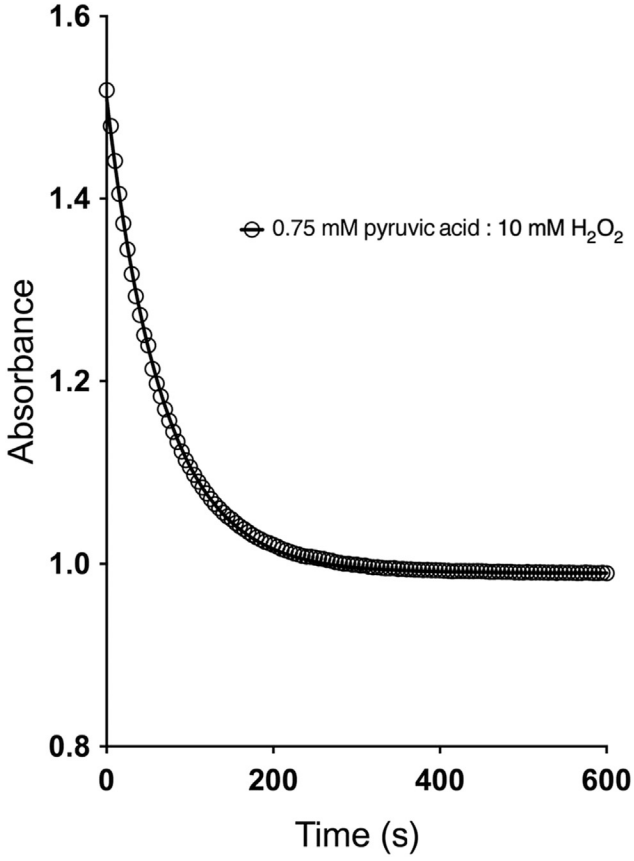

Figure 1. A representative plot showing the change in absorbance at 220 nm versus the time after mixing a solution of sodium pyruvate (0.75 mM) with H_2O_2 (10 mM) in 40 mM buffer phosphate, pH 7.4, ionic strength 0.15, at 25°C. The solid line through the data points represents the fit to a monoexponential or first-order loss.

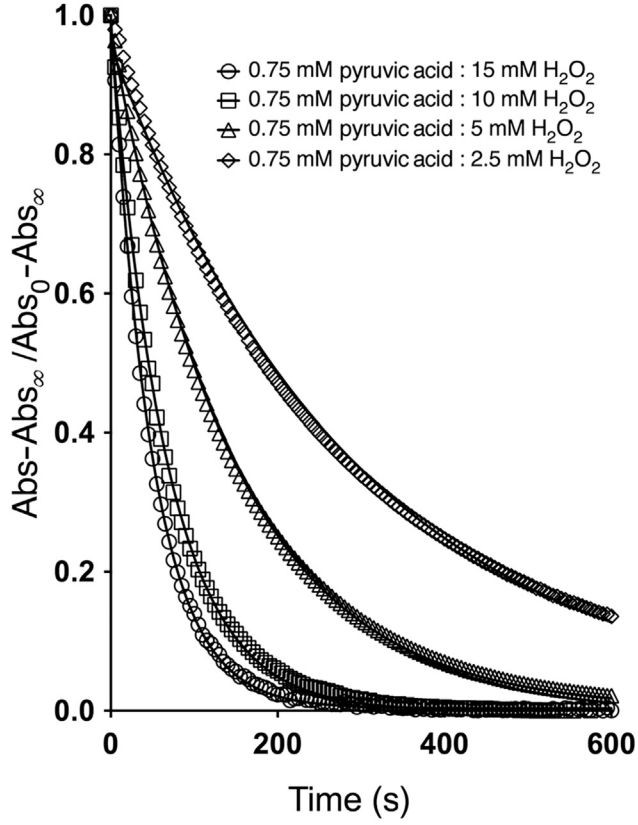

Figure 2. A representative graph indicating an overall drop absorbance at 220 nm from pyruvic acid decarboxylation in the presence of increasing concentrations of H_2O_2 (2.5-15 mM) at 40 mM buffer phosphate, pH 7.4, ionic strength 0.15 at 25°C. The absorbances reported on the y axes were normalized. The solid lines through the data points represents the fit to a monoexponential or first-order expression.

Gas Chromatography–Mass Spectrometric Analysis

The gas chromatography–mass spectrometric (GC-MS) data were collected on an Agilent 6890N gas chromatograph eluting into a Quattro Micro GC mass spectrometer (Micromass Ltd., Manchester, UK). A 15-m, 250-μm ID, 5% phenyl/methyl silicone capillary column (DB5-MS J&W Scientific) was used for separation with helium at constant flow of 1 mL/min (36 cm/s). Three microliter of sample in water solvent was injected onto the column in splitless mode with 0.7 min purge time. The injector port temperature was 240°C. The oven program was from 75°C to 300°C at 25°C/min. Electron impact ionization was used with ion energy of 70 V. The mass range was 45–410 m/z in 0.47 s. The quadrupole mass analyzer mass resolution was set to 0.6 μ FWHH.

Data Fitting

Data fitting to determine various rate constants values was performed using GraphPad/Prism version 6.0 (GraphPad Software, La Jolla, CA) using either nonlinear least-squares regression analysis or linear regression analysis. Nonlinear least-squares regression analysis with weighting (in order to minimize the weighted sum-of squares) was used to obtain best-fit values to the pH-rate profile of the second-order rate constant to pH.

Results and Discussion

The fast decarboxylation of pyruvate in aqueous solutions in the presence of different concentrations of H_2O_2 over a wide pH range between 2 and 9 at 25°C was investigated by UV spectrophotometry. Some selected kinetics data are shown in Figures 1 and 2. The speed of the reaction can be clearly seen by examining the half-lives for the reaction as seen in Table 1.

Under the conditions utilized, molar excess of H_2O_2 over pyruvic acid, the reactions followed pseudo first-order kinetics. The overall drop in absorbance at 220 nm because of the reaction of pyruvate with H_2O_2 could be described by a mono-exponential equation, Equation 1:

$$\mathrm{Abs} - \mathrm{Abs}_\infty = (\mathrm{Abs}_0 - \mathrm{Abs}_\infty)e^{-k_{obs}t} \quad (1)$$

where Abs_0 is the initial absorbance, Abs_∞ is the final absorbance at infinity, Abs is the absorbance at time, t, and k_{obs} is the pseudo first-order rate constant at each H_2O_2 concentration. By curve fitting the data to Equation 1, it was possible to experimentally determine the values of the observed rate constant, k_{obs}, under the specific conditions used.

Table 1
Half-Lives ($t_{1/2}$) for the Decarboxylation of Pyruvic Acid in the Presence of 5 and 10 mM H_2O_2 at pH 2 (HCl), and 5.5 and 7.4 (40 mM Buffer) at 25°C, and Ionic Strength 0.15

H_2O_2 Concentration (mM)	$t_{1/2}$ at pH 2 (min)	$t_{1/2}$ at pH 5.5 (min)	$t_{1/2}$ at pH 7.4 (min)
5	165	8.3	1.6
10	75	4.2	0.8

The $t_{1/2}$ is expressed in minutes.

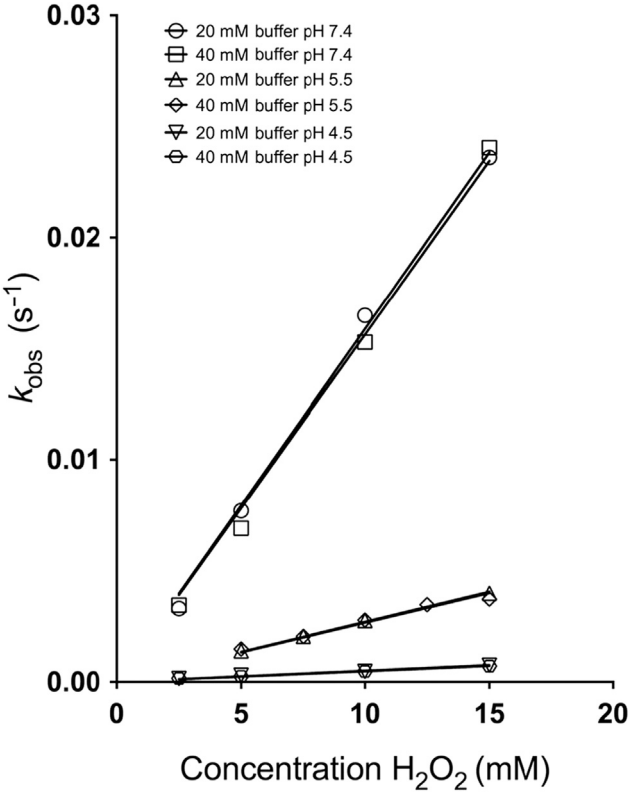

Figure 3. Observed pseudo first-order rate constants for the loss of pyruvate plotted against H_2O_2 concentration in phosphate buffer, 20 and 40 mM, at pH 7.4, and acetate buffer, 20 and 40 mM, at pH 5.5 and 4.5, ionic strength 0.15 M at 25°C. The slopes of each line represented the second-order rate constant k_{sec} at each pH value. Standard deviations were within the size of the symbol.

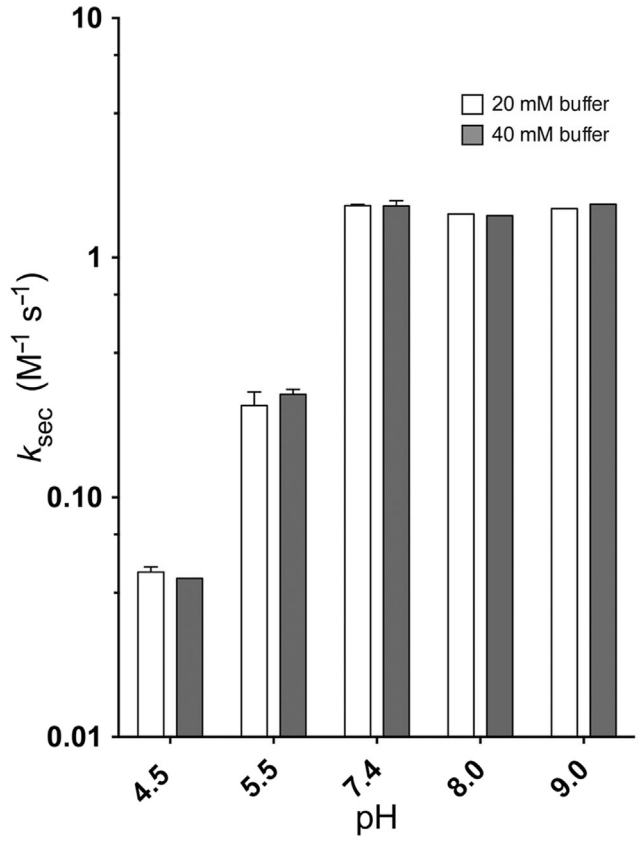

Figure 4. Impact of buffer concentrations on k_{sec} at 25°C. The results at each buffer concentration were reported as mean of two experiments.

By varying the molar excess of H_2O_2 relative to pyruvic acid, one could then test the relationship of the observed kinetics to H_2O_2 concentration. Assuming the reaction to be bimolecular, the overall loss of pyruvic acid (−dP/dt) might be described by Equation 2. In the presence of molar excess of H_2O_2, Equation 2 transforms to Equation 3:

$$-\frac{dP}{dt} = k_{sec}[P][H_2O_2] \quad (2)$$

$$-\frac{dP}{dt} = k_{obs}[P] \quad (3)$$

$$k_{obs} = k_{sec}[H_2O_2] \quad (4)$$

where k_{sec} is the second-order rate constant for the decarboxylation of pyruvic acid. One can therefore confirm the dependency on peroxide concentration and determine k_{sec} by plotting k_{obs} versus $[H_2O_2]$. Figure 3 shows representative examples of plots of k_{obs} values against the concentrations of H_2O_2 at various pH values. A linear dependency is seen. The plots pass through zero indicating that only the nucleophilic addition-decarboxylation reaction occurred during each experiment and that any endogenous reaction, reactions in the absence of added H_2O_2, were kinetically negligible. The impact of the buffer on the k_{sec} was evaluated performing the experiments at two different buffer concentrations, 20 and 40 mM between pH 4 and 9 (Figs. 3 and 4). The data showed that no buffer catalysis was observed at pH values between 4 and 9, indicating no proton transfer was occurring at the rate-determining step.

The reaction of pyruvic acid with H_2O_2 was confirmed by HPLC analysis. Figure 5 showed that acetic acid, retention time, Rt, approximately 8.2 min, was the degradation product at pH 7.4 value. Acetic acid was the degradation product at all pH values studied. The Rt values for acetic acid was confirmed by comparison with a standard.

A pH-rate profile for k_{sec} generated over a pH range of 2-9 is shown in Figure 6. This apparent sigmoidal plot could be fit to an empirical equation involving a simple ionization. When attempted (result not shown), an apparent pK_a value of about 6.3 results. Earlier work shows that the value of 6.3 could not correspond to

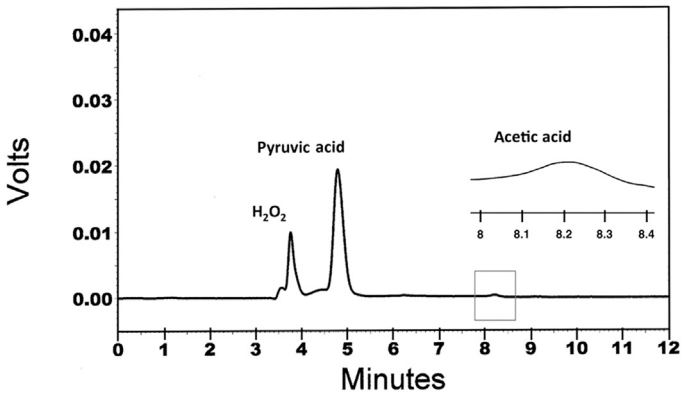

Figure 5. A representative HPLC chromatogram of pyruvic acid (1 mM) upon addition of H_2O_2 (1 mM) in buffer phosphate 40 mM, pH 7.4, IS 0.15 M, at 25°C.

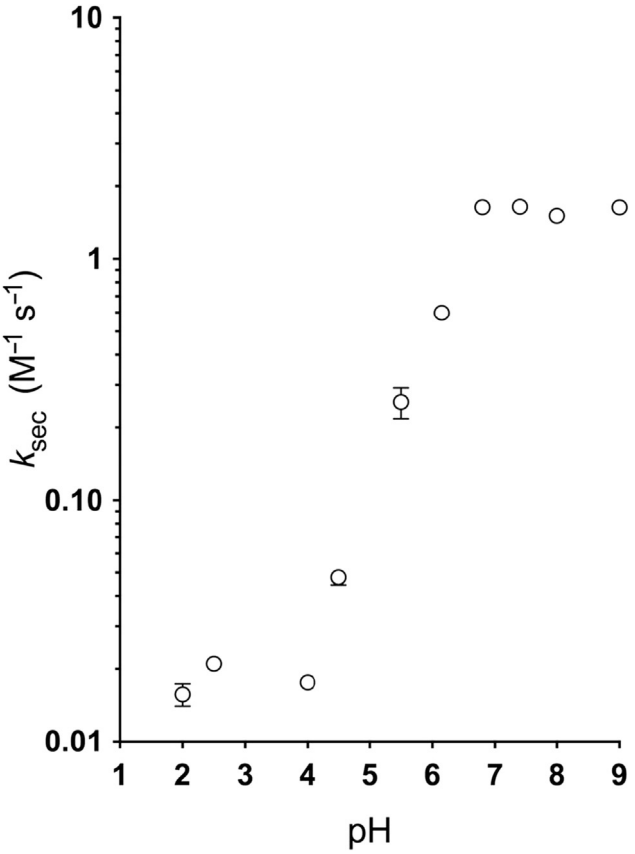

Figure 6. The pH dependence of the k_{sec} for decarboxylation of pyruvate in the presence of H_2O_2 at 25°C between pH 2 and 9. Experimental values were determined at 20 and 40 mM buffer concentration and 3 and 10 mM HCl and reported as mean value at each pH value.

any pK_a value associated with the various forms of pyruvic acid,[1] the dissociation of H_2O_2, pK_a >11.3,[19] or the peroxide addition product to pyruvic acid [pK_a = 2.5, calculated using Advanced Chemistry Development (ACD/Labs) Software V11.02 (©1994-2015 ACD/Labs)] (Scheme 1).

Although others have proposed, a very reasonable assumption, that peroxide driven decarboxylation of pyruvic acid and other α-keto carboxylic acids proceeds through an intermediate peroxide addition to the α-carbonyl (keto) group followed by the irreversible decarboxylation step as described in Scheme 1, no one has been able to adequately account for the pH dependency of the reaction and the molecular mechanism as pH is varied.[2–4,20]

The existence of a peroxide addition intermediate to oxopyruvic acid proposed by others is consistent with the findings here. This intermediate is not specifically detectable by normal analytical techniques, although Asmus et al.[21] do appear to detect the species in mixtures of deuterium water and deuterium methanol, applying the combination of low temperature and a ^{13}C-NMR technique. As a model for the addition, the nucleophilic addition of H_2O_2 to ethyl pyruvate was evaluated using ^{1}H and ^{13}C-NMR in water solutions at 25°C and pH 5. The ^{1}H-NMR and ^{13}C-NMR spectra (Fig. 7) of ethyl pyruvate in aqueous solutions showed the presence of the peaks arising from the hydrogens and carbons associated with the oxo and hydrated forms, as was found in a previous study with pyruvic acid in water solutions.[1] After having added an excess of H_2O_2 relative to the ester concentration, the appearance of new peaks were observed that corresponded to the proton and carbon signals of the hydroperoxide adduct at the carbonyl site (ethyl-2-hydroperoxy-2-hydroxypropanoate) (Fig. 7). The relative positions of the peaks were in agreement with the assignment. HSQC and HMBC investigations confirmed the structure of the hydroperoxide adduct (Fig. 8). The addition was also confirmed by GC-MS analysis of the sample (Fig. 9).

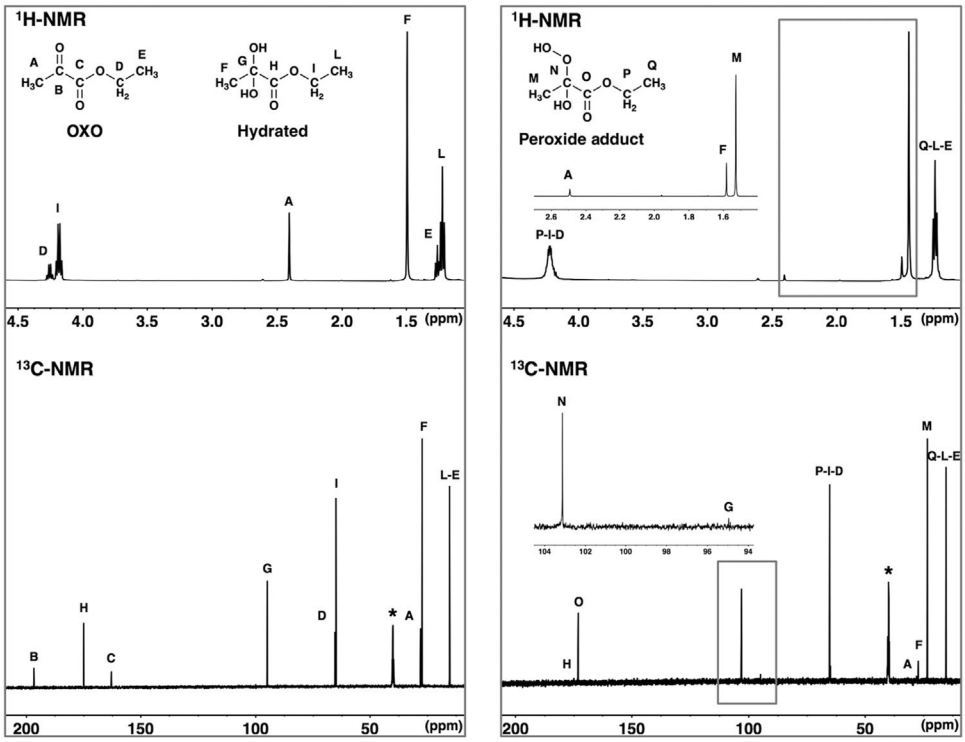

Figure 7. ^{1}H-NMR and ^{13}C-NMR spectra of ethyl pyruvate at pH value 5 (left) and after mixture with H_2O_2 (right). Chemical shift for protons were referred to water signal and chemical shift for carbons were referred to DMSO-d_6 (*) as internal standard.

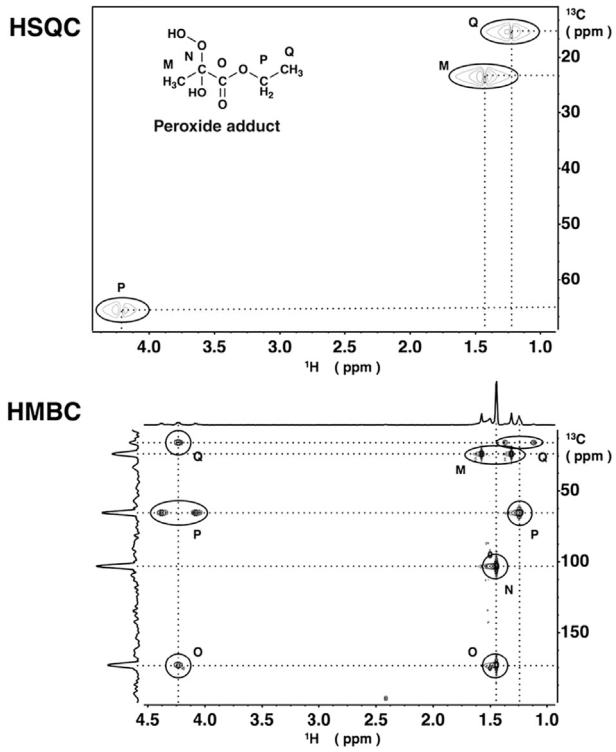

Figure 8. 2D ^{1}H-^{13}C-NMR spectra of a solution of ethyl pyruvate and H_2O_2 in water at pH 5, IS 0.15, at 25°C. The cross-peaks displayed by 2D NMR were used to identify the structure of the intermediate (HSQC), including the correlation of the chemical shifts of protons and carbons separated from each other with two and three chemical bond (HMBC).

From Figure 9, one can see the characteristic peaks m/z 150.2 associated with the hydroperoxide adduct with a m/z 116.1 associated to the oxo form of the ethyl pyruvate. This confirms that the ethyl ester form of pyruvate can react with H_2O_2 in water

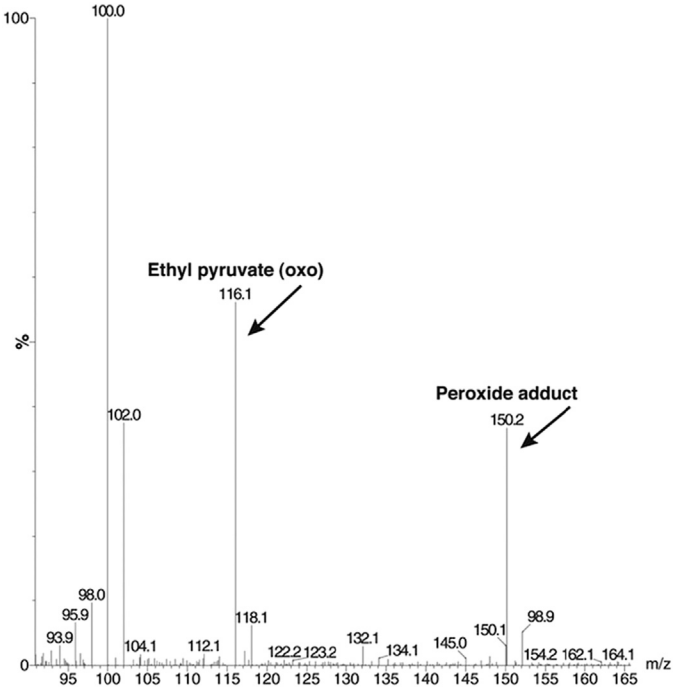

Figure 9. Gas chromatography–mass spectrometric analysis of a solution of ethyl pyruvate and H_2O_2 in water at pH 5, ionic strength 0.15, at 25°C.

Table 2
Percent (%) of Oxo, Hydrated, and Peroxide Adduct of Ethyl Pyruvate (75 mM) in the Presence of 75–225 mM H_2O_2, at 25°C, pH 5, and Ionic Strength 0.15

H_2O_2 Concentration (mM)	Oxo (%)	Hydrated (%)	Peroxide Adduct (%)
75	16.2	41.1	42.7
150	10.7	26.9	62.4
225	7.8	19.5	72.7

The percent of each form was determined from the integration of the respective methyl protons adjacent to the α-carbonyl of ethyl pyruvate.

solutions and form a stable nucleophilic adduct.[22] On the basis of the results from an earlier study on the hydration of pyruvic acid under acidic pH conditions,[1] the hydrated form of the ethyl ester was more stable than the oxo form. From the integration of the methyl hydrogens adjacent to the a-carbonyl group, it was possible to determine the percent of hydrated form for the ester to be 74%, a value similar to what is seen with protonated form of pyruvic acid under acidic pH conditions.[1] After having added different concentrations of H_2O_2, the percent of oxo and hydrated changed, but as expected, the ratio did not change. In the presence of increasing concentrations of H_2O_2, the percent of peroxide adduct increased, whereas the hydrated and the oxo forms decreased (Table 2).

If one were to estimate the equilibrium constants for the peroxide and water addition, the peroxide addition is about 800 times more favorable if one assumes the water concentration to be 55.5 M. These observations with ethyl pyruvate experimentally confirm H_2O_2 addition to a pyruvic acid species. Pyruvamide was also studied and similar results were observed (data not presented) as it was found that pyruvamide was chemically unstable in peroxide solutions undergoing both a polymerization reaction as well as probable N-oxide formation with time.

Referring to Scheme 1, one can assume that the ionization of the carboxylic acids groups of the hydrated and oxo forms of pyruvic acid are instantaneous. Although the kinetics of hydration and dehydration of pyruvic acid is not instantaneous, as one is able to see separation signals by NMR for various protons and carbons for the hydrated and oxo forms of pyruvic acid,[1] the reaction kinetics is fast enough that the reactions are complete in a matter of a few seconds or less (unpublished results from our laboratory).

To be able to describe the observed pH-rate profile in the pH range of 4-9, Scheme 2 is proposed. Earlier studies[1] have shown that at pH values between 4 and 9, the oxo form of pyruvic acid was more than 99.9% in its deprotonated form (pK_a^{oxo} ~ 1.7) and that pyruvic acid overall was 90% or higher in the oxo, or non-hydrated form in this pH range. On the basis of unpublished studies on the dimerization and polymerization of pyruvic acid in water solution (a follow-up paper under preparation), no significant enol form or dimer of pyruvic acid were present during the analyses. Therefore, between pH 4 and 9, the reactive species involved in the formation of the peroxide intermediates was the oxo form of pyruvate.

To account for the pH dependency of k_{sec}, it is proposed (Scheme 2) that kinetically the first step in this pH range is the nucleophilic attack of the anion of H_2O_2, HOO^-, on the electrophilic carbon of the α-keto group of pyruvate to form the tetrahedral intermediate I′. I′ was formed with a rate constant k_1. Between pH 4 and 9, the oxygen anion of the intermediate I′ is instantaneously protonated to the alcohol form, I″. The intermediate I″ is then converted to products, CO_2, water and acetic acid in a second step, with a rate constant k_2 (Scheme 2). The intermediate I′ could also regenerate the reactive species, pyruvate, and HOO^- with a rate constant k_{-1}.

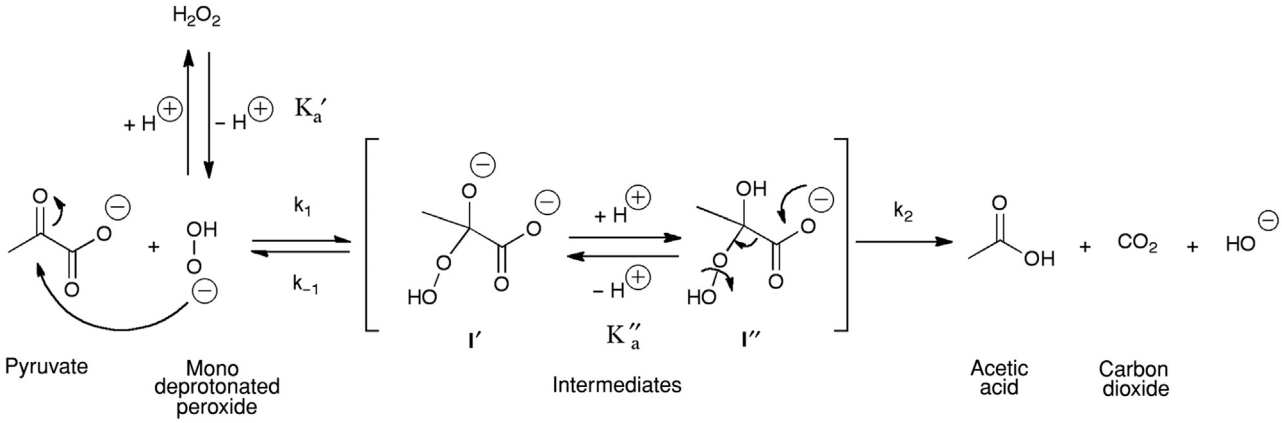

Scheme 2. Proposed pathway for the reaction of pyruvate with the H_2O_2 between pH 4 and 9 consistent with the pH-rate profile and the lack of observed buffer catalysis. The reaction proceeds via the reversible formation of tetrahedral intermediate I′, its protonation to I″, and subsequent irreversible decarboxylation.

Assuming Scheme 2, the rate of product formation, CO_2, is illustrated here as could acetic acid, can be defined by Equation 5:

$$\frac{d[CO_2]}{dt} = k_2\left[I''\right] \tag{5}$$

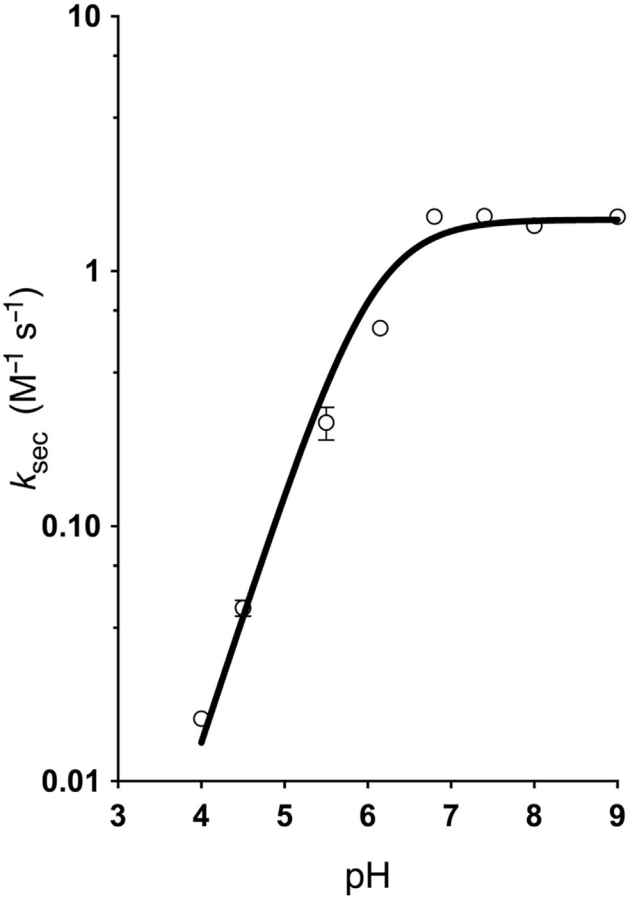

Figure 10. The pH dependence of the k_{sec} for decarboxylation of pyruvate by H_2O_2 at 25°C between pH 4 and 9. Experimental values were determined at 20 and 40 mM buffer concentration and reported as mean value at each pH. The solid line was obtained by fitting the results to Equation 10.

Making the steady-state approximation (SSA) for the concentration of the reactive intermediate I″ being low and constant during the reaction results in Equation 6:

$$\frac{d\left[I\right]}{dt} = k_1\left[HOO^-\right]\left[P\right] - k_{-1}\left[I'\right] - k_2\left[I''\right] \tag{6}$$

Making the SSA, the variation of the concentration of the intermediates d[I]/dt is assumed to be zero resulting in Equation 7:

$$\left[I''\right] = \frac{k_1[P]\left[HOO^-\right]}{k_{-1}\frac{K''_a}{[H^+]}} + k_2 \tag{7}$$

where K''_a is the dissociation constant of I′ defined by Equation 8:

$$K''_a = \frac{[H^+]\left[I''\right]}{[I']} \tag{8}$$

Substitution of Equations 7 and 8 into Equation 5 gives Equation 9:

$$\frac{d[CO_2]}{dt} = \frac{K'_a k_1[P][H_2O_2]}{\frac{k_{-1}K''_a}{k_2} + [H^+]} \tag{9}$$

where K'_a is the dissociation constant of H_2O_2 ($pK'_a > 11.3$).[19] Therefore, the second-order rate constant for the reaction of H_2O_2 with pyruvate, k_{sec}, can be reduced to Equation 10.

$$k_{sec} = \frac{K'_a k_1}{\frac{k_{-1}K''_a}{k_2} + [H^+]} \tag{10}$$

The k_{sec} defined in Equation 10 represented a complex rate constant made up of various microconstants and various dissociation constants. That is, it incorporates 3 rate constants (2 for the reverse addition of the nucleophilic specie HOO^- to pyruvate and 1 for the irreversible decarboxylation) and 2 dissociation constants (one for H_2O_2 and one for the intermediate I″). Also, Equation 10, and thus estimates of the various microrate constants, assumes that all of the pyruvic acid is 100% in the oxo form and is invariant as pH changes. As stated earlier, at pH values at 4, pyruvic acid is 90% in its oxo form changing to 95% at higher pH values. The small change is assumed to be negligible and thus no corrections were attempted here.

A similar pathway/model was proposed earlier but no experimental data were available regarding the nature of intermediates

I′ and I″.[2] On the basis of an elegant carbon kinetic isotope effect experiment,[4] it was demonstrated that the rate-limiting step of the reaction was pH dependent with possible change in rate-determining step. The model proposed here is consistent with the work of Melzer and Schmidt.[4]

Scheme 2 and the derived mathematical model can explain the mechanism of reaction in the pH range between 4 and 9 (Fig. 10). This model is also consistent with the observation of no buffer catalysis. That is, between pH 4 and 6 where the rate increased sharply with pH is because of increase in concentration of the nucleophilic species HOO^-, the monodeprotonated form of H_2O_2.

In this pH range, when $[H^+] > > (k_{-1}K''_a/k_2)$, Equation 10 simplifies in Equation 11:

$$k_{sec} = \frac{K'_a k_1}{[H^+]} \tag{11}$$

Thus, the reaction appears to be specific base catalyzed with k_1 representing the rate-determining step.

From pH 7 to 9, k_{sec} was constant and independent of pH. This can be explained by assuming the rate-determining step changed so that the reversible addition of HOO^- was fast and the decarboxylation became rate determining.

Thus, at pH values greater than 7, k_{sec} could be described by Equation 12:

$$k_{sec} = \frac{K'_a k_1 k_2}{k_{-1}K''_a} \tag{12}$$

where k_2 is now rate determining with the addition of the peroxide to the pyruvic acid being defined by the equilibrium constant, k_1/k_{-1}.

At the inflection point, around pH 6.3, the $[H^+]$ corresponded to the ratio of the rate constants of breakdown of the carbonyl-peroxide adduct I′ and decarboxylation of I″, multiplied by the dissociation constant of the tetrahedral intermediate I″. This inflection point corresponds to the apparent pK_a value of 6.3 described earlier from an empirical fit.

$$\left[H^+\right] = \frac{k_{-1}K''_a}{k_2} \tag{13}$$

The mechanism of reaction involving the formation of the tetrahedral intermediate was supported from the literature[17,18] as well as the experimental observations seen here.

By curve fitting the experimental data, to Equation 10, the rate constant k_1 was estimated to be equal to 3.5×10^5 M^{-1}/s by assuming that K'_a has a value of $10^{-11.3}$. The estimated value of k_1 depends on the value used for K'_a. The other constants, k_{-1} and k_2, could not be estimated from the fitting.

Because the reaction of pyruvic acid and H_2O_2 was found to be slower at pH 2, a ^{1}H-NMR experiment was performed to follow the disappearance of the two peaks for pyruvic acid from the methyl hydrogens for the hydrated and oxo form (1.45 and 2.25 ppm, respectively) and the appearance of acetic acid (1.8 ppm) during the time following mixing with H_2O_2 with pyruvic acid. From previous studies, at pH 2, the percent of oxo form was slightly more than the percent of hydrated form.[1] Even though the kinetics were relatively slow at pH 2, one could not observe any peaks corresponding to the intermediate, supporting the SSA made to describe the kinetics above pH 4. A ^{13}C-NMR kinetic experiment of pyruvic acid and H_2O_2 was also attempted at pH 2. In this case, one could not follow the reaction accurately during the time because it was still quite fast. However, the spectra did confirm the expected peaks for both the degradation products, acetic acid (20 and 176 ppm) and carbon dioxide (124 ppm). The carbon dioxide peak gradually disappeared because of evaporation.

At pH values below 4, the second-order rate constant for the decarboxylation reaction becomes approximately pH independent; however, because the state of ionization and hydration changes significantly in this pH range, one can imagine an alternative and more complex pH dependency. No attempt was made to explore the specifics of the mechanism and what was the rate-limiting step in this pH range. Similar reactants and the intermediates could exist in various ionic forms and the percent of hydrated form increased.

Conclusions

UV spectrophometry was successfully employed to study the fast kinetics of pyruvate in aqueous solutions in the presence of H_2O_2. Combining HPLC and NMR analyses, it was possible to confirm the formation of the degradation products acetic acid and CO_2. A proposed mechanism of reaction involving a change in rate-determining formation of tetrahedral intermediate species to rate-determining decarboxylation could explain the pH-rate profile between pH 4 and 9.

Acknowledgments

The authors would like to thank Dr. Todd D. Williams and Bob Drake from Mass Spectrometry and Analytical Proteomics Laboratory at The University of Kansas for their valuable technician assistance. Support for the NMR instrumentation was provided by NIH Shared Instrumentation grant #S10RR024664, #S10RR014767, and NSF Major Research Instrumentation grant #0320648. The QuattroMicro GC-MS was purchased with support from NIH SIG S10 RR019398.

References

1. Lopalco A, Douglas J, Denora N, Stella VJ. Determination of p*K*a and hydration constants for a series of α-keto carboxylic acids using nuclear magnetic resonance spectrometry. *J Pharm Sci*. 2016;105:664-672.
2. Hamilton GA. The proton in biological redox reactions. *Progr Biorganic Chem*. 1971;1:83-157.
3. Perera A, Parkes HG, Herz H, Haycock P, Blade DR. High resolution ^{1}H NMR investigations of the reactivities of alpha-keto acid anions with hydrogen peroxide. *Free Rad Res*. 1997;26:145-157.
4. Melzer E, Schmidt HL. Carbon isotope effects on the decarboxylation of carboxylic acids. Comparison of the lactate oxidase reaction and the degradation of pyruvate by H_2O_2. *Biochem J*. 1988;252:913-915.
5. Hovorka S, Schoneich C. Oxidative degradation of pharmaceuticals: Theory, mechanism and inhibition. *J Pharm Sci*. 2001;90(3):253-269.
6. Wu Y, Levons J, Narang AS, Raghavan K, Rao VM. Reactive impurities in excipients: profiling, identification and mitigation of drug-excipient incompatibility. *AAPS Pharm Sci Tech*. 2011;12(4):1248-1263.
7. Narang AS, Rao VM, Desai DS. Effect of antioxidants and silicates on peroxides in povidone. *J Pharm Sci*. 2012;101(1):127-139.
8. Ha E, Wang W, Wang J. Peroxide formation in polysorbate 80 and protein stability. *J Pharm Sci*. 2002;91(10):2252-2264.
9. Herman AC, Boone TC, Lu HS. Characterization, formulation, and stability of neupogen (filgrastim), a recombinant human granulocyte-colony stimulating factor. In: Pearlman R, Wang YJ, eds. *Formulation, characterization, and stability of proteins drugs*. Vol 9. New York: Plenum Press; 1996:303-328.
10. Knepp VM, Whatley JL, Muchnik A, Calderwood TS. Identification of antioxidants for prevention of peroxide-mediated oxidation of recombinant human ciliary neurotrophic factor and recombinant human nerve growth factor. *J Pharm Sci Technol*. 1996;50:163-171.
11. Azaz E, Donbrow M, Hamburger R. Incompatibility of nonionic surfactants with oxidisable drugs. *Pharm J*. 1975;211:15.
12. Coates LV, Pahley MM, Tattersall K. The stability of antibacterials in polyethylene glycol mixtures. *J Pharm Pharmacol*. 1961;13:620-624.
13. James KC, Leach RH. The stability of chloramphenicol in topical formulations. *J Pharm Pharmacol*. 1970;22:607-611.
14. Hartauer KJ, Arbuthnot GN, Baertschi SW, et al. Influence of peroxide impurities in povidone and crospovidone on the stability of raloxifene

hydrochloride in tables: identification and control of an oxidative degradation product. *Pharm Dev Technol*. 2000;5(3):303-310.
15. Stella VJ. Chemical drug stability in lipids, modified lipids, and polyethylene oxide-containing formulations. *Pharm Res*. 2013;30:3018-3028.
16. Narang AS, Desai D, Badawy S. Impact of excipient interactions on solid dosage form stability. *Pharm Res*. 2012;29:2660-2683.
17. Waterman KC, Adami RC, Alsante KM, et al. Stabilization of pharmaceuticals to oxidative degradation. *Pharm Dev Technol*. 2002;7(1):1-32.
18. Das UN. Is pyruvate an endogenous anti-inflammatory molecule? *Nutrition*. 2006;22:965-972.
19. Prankerd RJ. Data Compilations. Appendix A. Main list. In: Brittain HG, ed. *Profile of drug substances, excipients, and related methodology*. 1st ed Vol 33. London, UK: Academic Press; 2007:213.
20. Bunton CA. Oxidation of α-diketones and α-keto-acids by hydrogen peroxide. *Nature*. 1949;163:444.
21. Asmus C, Mozziconacci O, Schoneich C. Low temperature NMR characterization of the reaction of sodium pyruvate with hydrogen peroxide. *J Phys Chem A*. 2015;119(6):966-977.
22. Ajami AM, Sims CA, Fink MP. 2005. Pyruvate ester composition and method of use for resuscitation after events of ischemia and reperfusion. Patent US 6846842 B2.